PPPL--2735

DE91 010011

Quenching of Einstein-coefficients by photons.

F. Aumayr[a] , W. Lee, C. H. Skinner[b], and S. Suckewer[b]

Mechanical and Aerospace Engineering Department,

Princeton University

Princeton, New Jersey 08544, USA

Abstract

Experimental evidence is presented for the change of Einstein's A-coefficients for spontaneous transitions from the upper laser level of an argon ion laser discharge due to the presence of the high-intensity laser flux. To demonstrate that this quenching effect cannot be attributed to a reduction in self-absorption of the strong spontaneous emission line, absorption and line profile measurements have been performed. Computer modelling of the reduction of self absorption due to Rabi splitting also indicated that this effect is too small to explain the observed quenching of spontaneous line emissions.

I. INTRODUCTION

Experimental evidence for quenching of Einstein's A-coefficients has been presented in several recent papers.[1-3] A change in branching ratios of spontaneous emission lines was found to occur both in laser produced plasmas as a function of electron density,[1,2] as well as inside a laser cavity as a function of laser photon flux.[3]

In laser produced carbon plasmas this change amounted to almost an order of magnitude [e.g., branching ratio of CIV 3p→3s (580.1 - 581.2 nm) and 3p→2s (31.2 nm) transitions] when the electron density changed from approximately $N_e \approx 10^{18}$ cm^{-3} to 10^{19} cm^{-3}. This could also be observed in CIII for the 3d→3p (569.6 nm) and 3d→2p (57.4 nm) transitions and in NV for the 3p→3s (460.3 - 462.3 nm) and 3p→2s (20.9 nm) transitions.[2] Inside an argon ion laser cavity only a 10% change in branching ratio between the spontaneous emission lines ArII 399.21 nm ($4p\ ^4D^o_{5/2} \rightarrow 3d\ ^4D_{3/2}$) and ArII 442.60 nm ($4p\ ^4D^o_{5/2} \rightarrow 4s\ ^4P_{3/2}$) could be measured[3] during lasing of the 514.53 nm transition ($4p\ ^4D^o_{5/2} \rightarrow 4s\ ^2P_{3/2}$).

Since then several attempts have been made to explain these effects theoretically. Chen and Lebowitz[4] suggested that the phenomenon observed in laser produced plasmas is due to weak trapping of plasma electrons into highly excited states of the radiating ions. In the case of such trapping low frequency lines might be strongly shifted and, therefore, not observable. Of course, this explanation would not be applicable to the results obtained in the low density gain medium inside the laser cavity. On the other hand, Griem has proposed an explanation[5] based on Rabi oscillations solely for the quenching effect observed in the high intensity argon ion laser field. His approaches will be examined in Sec. III of this paper.

Not a theory but a simple hypothesis that would be applicable to both experiments was given in Ref. 3. If the spontaneous emission of an atom or ion would rather depend on dynamic effects like collisions, this could qualitatively (but not, of course, quantitatively) explain the observable effects. In the case of the high density laser produced plasma, inelastic electron collisions with atoms or ions might have a significant disruptive effect on their spontaneous emission, which means that the change of emissivity should depend on the ratio of collisional frequency ν_{coll} to the frequency of spontaneous emission from level n: $\nu_n \approx A_n = \sum_{k<n} A_{nk}$ where subscript nk indicates transitions between level n and levels k<n. Indeed, for a plasma with $T_e \approx 5$ eV and $N_e \approx 10^{19}$ cm^{-3} the frequency, ν_{coll} , is approximately 10^3 times larger than ν_n for the 3p level of CIV. One would also expect a larger disruptive effect for weaker transitions, therefore, a larger change in A-value should occur for the 3p → 3s than for the 3p → 2s transition whose A-coefficient is about 150 times larger than that of the 3p → 3s transition. This leads to observable changes in the branching ratio.

A much more important implication of our hypothesis is that collisions of photons with atoms or ions, should also provide quenching of Einstein coefficients if the frequency of such collisions is sufficiently high. For a maximum intra-cavity power density of approximately 5 kW/cm^2 and a typical ion laser line width of 5 GHz for the 514.53 nm lasing line the stimulated emission frequency in Ref. 3 (calculated as the Einstein B-coefficient for stimulated emission times the spectral energy density of the laser) is estimated to exceed the total spontaneous emission frequency for the 4p $^4D^o_{5/2}$ level by about a factor of 100. Extrapolating the results of the laser plasma experiment,[1,2] therefore, an observable quenching effect can be expected for lines differing in A-coefficient by a factor of 50.

This paper deals with new, more elaborate investigations of the quenching effect inside an argon ion laser cavity of ArII emission lines and also presents new results on ArII absorption as well as line profile measurements. Experimental details of the emission and absorption measurements are given in Sec. II.A and II.B, respectively. Line profile measurements and the role of Rabi splitting in the emission and absorption data is discussed in Sec III. Section IV presents a summary of our results.

II. THE EXPERIMENT

A. Emission measurements

The experimental setup used in the emission measurements is shown in Fig. 1(a). The CW argon ion laser is tuned to a particular lasing line by changing the position of the 100% reflectivity mirror and the angle of the prism in front of the mirror. In this way it is possible to control the photon density in the discharge over a very large range and, therefore, change the photon-ion collision frequency without any significant change of the gas or plasma parameters in the discharge.

An argon ion laser was chosen because ArII has a number of lasing lines and appropriate non-lasing lines in a convenient (visible) spectral range. For example, the upper level 4p $^4D^o_{5/2}$ of the ArII 514.53 nm lasing line is a common upper level for seven non-lasing transitions[6,7] (see Fig. 2) whose A - coefficients differ by up to a factor of 50. Similar conditions hold for the ArII 487.99 nm (4p $^2D^o_{5/2} \rightarrow$ 4s $^2P_{3/2}$) lasing line. Both lasing transitions share a common lower level.[8] This lower lasing level decays very rapidly by spontaneous emission to the ground level $3p^5$ ^2P with a rate $A = 2.7 \times 10^9\ s^{-1}$. The fast decay of the 4s $^2P_{3/2}$ level (resulting in the low population of this level) is the primary cause of the creation of the population inversion rather

than a selective population of upper lasing level 4p $^4D^o_{5/2}$. In addition, the transitions between the 4s $^2P_{3/2}$ level and lower levels of non-lasing transitions (4s ^4P, 3d ^4D, and 3d ^4F) are intercombination transitions and, therefore, have quite low radiative transition probability. Hence, one should not expect to see any significant change of population of these 4s ^4P, 3d ^4D, and 3d ^4F levels due to lasing action to the 4s $^2P_{3/2}$ level. This is a very important and unique feature of the argon ion laser and makes this laser an almost ideal one for our experiment.

The argon ion laser (Innova 200) had a maximum output beam power of about 9 W at the 514.53 nm lasing line and about 7 W at 487.99 nm which was constantly monitored by an internal power meter. The length of the discharge tube was L = 1.57 m, its effective diameter was d ≈ 2 mm and the output mirror had a transmissivity of 5% at 514.53 nm. Therefore, an intra-cavity power density of approximately 6 kW/cm^2 for the 514.53 nm lasing line (electric field strength of about 1.5 kV/cm) could be achieved.

A dichroic filter with low transmission at the lasing wavelengths and relatively high transmission elsewhere was utilized to block the laser lines right after the output mirror. In our experimental setup, light from the argon ion laser was directed by a set of mirrors towards the entrance slit of a 0.5 m Czerny-Turner monochromator (SPEX - 1870) with a 2400 gr/mm holographic grating. As an example line spectra obtained in two spectral regions are shown in Fig. 3.

By tuning the cavity to obtain lasing action at 514.53 nm a change in the 4p $^4D^o_{5/2}$ upper level population resulted in a decrease of the intensity of the spontaneous emission lines to the 4s ^4P, 3d ^4D, and 3d ^4F levels (see e.g., Fig. 3). Since these intensities are proportional to the upper level population, all emission lines should exhibit the same decrease. However, in our

measurements each line yields a different "apparent" depopulation of the 4p $^4D^o_{5/2}$ upper level as can be seen from Fig. 4.

In this figure the ratios of emission intensities at the maximum achievable intra-cavity power density to emission intensities at zero intra-cavity power density for different spontaneous emission lines are shown. Since the volume averaged 4p $^4D^o_{5/2}$ population can only have a single value, our data indicate a monotonic dependence on the Einstein A-coefficients of the respective transitions. From Fig. 4 and earlier results [3] it is obvious that there is no smooth dependence on wavelength. The largest discrepancy in apparent depopulation (22.4% ± 1.0 and 30.7% ± 1.0) was found between the strongest (442.6 nm) and weakest (399.2nm) transition from this upper level (cf. Fig 3). In Fig. 5 the branching ratio between the 399.2 nm and the 442.6 nm transition (whose A-coefficients differ by a factor of 54) is plotted as a function of intra-cavity power density showing a decrease of the branching ratio with increasing 514.53 nm photon flux inside the argon ion laser cavity (in Fig. 5 the branching ratio is normalized to 1 for a discharge without lasing (detuned laser cavity).

In extremely careful examinations, including several supplementary experiments, possible explanations for these findings were investigated:

a) Different spectrometers equipped with photomultiplier tubes or multichannel detection systems were used and tested for a possible nonlinear response at low and high signal intensities. No such influence could be detected.

b) The identification of the different lines was checked very carefully (the resolution of our monochromator was 0.027 nm FWHM, cf Fig. 3). The background signal from residual lasing radiation inside the

monochromator was found to be negligible due to the dichroic filter used to block the lasing line.

c) No shift in wavelength or line broadening could be observed within the wavelength resolution of our monochromator when tuning the laser cavity to 514.53 nm. Higher resolution line profile measurements using a Fabry-Perot interferometer will be described in Sec. III.A. Possible effects of Rabi oscillations on line intensities as proposed in Ref. 5 will be discussed in more detail in Sec. III.B.

d) Optical components in the beam path like mirrors, filters, etc. might at least in principle change their (wavelength dependent) reflectivity or transmissivity when hit by intense (9 W) laser radiation. Critical components like the dichroic filter (used to block the lasing line) and the cavity output mirror where investigated by illuminating them simultaneously with 400 nm dye and 514.53 nm ArII laser radiation. No change in. transmissivity within the experimental errors of ±0.5% could be detected. Additional evidence is illustrated in Fig. 3. No change in the intensities of the neighboring lines of 442.6 nm and 399.2 nm during lasing could be found.

e) By inserting a rotatable Glan-Taylor prism polarizer into the beam path it could be demonstrated, that the apparent depopulation did not depend on the polarization of the spontaneous emission lines (cf. Fig. 6).

f) Different observation geometries, i.e., observation in a backward direction [via reflection on the prism surface; cf. Fig. 1(b)] and intra-cavity observation with a small diameter optical fiber (aligned under a slight angle to the laser beam axis) resulted in the same "quenching" effect.

g) Our most serious concerns were dedicated to the problem of self-absorption of the spontaneous emission lines. Of course, a 1.57 m long argon ion laser plasma tube (gas fill pressure 300 mTorr) cannot be treated as optically thin, and self-absorption is expected especially for the strong transitions. On the one hand, a change in absorption with lasing action could, in principle, lead to results as shown in Fig. 5 if the intensity of the 399.2 nm line would decrease (due to an increase in absorption) and the intensity of the 442.6 nm line would stay constant (saturated intensity) while the intracavity power is increased. On the other hand, with a changed A-coefficient (cf. our hypothesis in Sec. I) we should also observe a change in the absorption B-coefficient, otherwise the thermodynamic relation between the A- and B- Einstein coefficients would be violated. Absorption measurements were, therefore, absolutely necessary and are described in the following section.

B. Absorption measurements

In our emission experiments we compare only intensities with and without lasing action while the laser discharge current, fill pressure, etc. stay constant. Therefore, only a change in absorption with lasing action can affect our results. This could arise from changes in the line shape due to Rabi splitting (discussed further in Sec. III) or by a collisional interaction of the lower lasing level 4s $^2P_{3/2}$ (whose population should increase during lasing at 514 nm) with the lower levels of the spontaneous emission lines. However, as was indicated earlier, this level decays to the argon ion ground state $3p^5\ ^2P$ with a large transition rate, hence, its population should always be small. The change introduced in level population by the intra-cavity field can be estimated by following the paper of Johnston.[10] Assuming an initial (i.e., without lasing) inversion ratio of N_u^o/N_l^o = (2 - 3) (cf. Ref. 7) between the 4p $^4D^o_{5/2}$ upper

level (u) and the 4s $^2P_{3/2}$ lower lasing level (l), the fractional lower level population increase denoted by $(N_l^f - N_l^o)/N_l^o$, where N_l^f is the population with lasing, can be calculated from the fractional upper level population decrease $(N_u^o - N_u^f)/N_u^o$, the level decay rates τ_u, τ_l and the spontaneous emission rate A_{ul} (Ref. 10). Due to the large transition rate τ_l of the lower laser level to the ArII ground state a 20% decrease in upper level population results in a lower level population increase of less than 3%, too small to account for a significant increase in the lower level population of the non-lasing transitions via nonradiating transitions (radiative transition rates from the 4s $^2P_{3/2}$ level to lower non-lasing levels are small due to intercombination character of these transitions). Furthermore, no change in spontaneous emission line intensity from the 4p $^4D^o_{5/2}$ level could be observed when tuning the laser to the 487.99 nm lasing line, which has the same 4s $^2P_{3/2}$ lower level as the 514.53 nm line.

In addition, we repeated our emission measurements using different argon ion laser with shorter discharge tubes (0.90 m and 1.2 m) and different output mirrors. Within our experimental errors all lasers yielded the same apparent depopulation when compared at the same intra-cavity intensities, although especially the opacity of the 442.6 nm emission line was considerably different in each case (absorption of 442.6 nm probing radiation changed from 45% for the 0.9m discharge to 85% for the 1.57m discharge).

To check whether the observed 10% quenching effect can be attributed to a change in self-absorption of the different spontaneous emission lines, absorption measurements with quite low accuracy (±3%) are sufficient. To observe a change in the absorption B-coefficient, as suggested by thermodynamic considerations, requirements on the accuracy of the absorption measurements are much more stringent. Such a change would be of the order

of only 2% (10% effect of quenching for the 399.2 nm line with 25% absorption; cf. the results of the absorption measurements for 399.2 nm below).

First we measured absorption of the 399.2 nm line with 395 - 405 nm probing radiation from a Coherent 599 dye laser (Exalite 400E dye and stilbene-1 dye laser optics yielded 10 mW tunable dye output). No change in absorption within the experimental error of ±2% could be observed. Since further attempts to improve the accuracy of these measurements were unsuccessful (e.g., we tried to use a double pass through the absorbing medium) we built the experimental setup shown in Fig. 1(b). Spontaneous emission light from a second argon ion laser was mechanically chopped and injected into the first argon ion laser cavity through the output coupler. After passing through the absorbing medium the attenuated probing radiation was partially reflected from the intra-cavity prism surface and guided by a set of mirrors to the monochrometer. Dichroic filters as described in Sec. II.A were appropriately positioned. A lock-in amplifier was used to distinguish the probing radiation from the light of the investigated laser. Considerable absorption (85%) was found for the strong transition at 442.6 nm, whereas absorption was small (25%) for the weakest transition at 399.2 nm. Since the prism and the high reflector were on the same mount, lasing had to be achieved by fine-tuning of the output coupler instead of the high reflector. In Fig. 7(a) we show the transmitted fraction (75%) of the probing radiation in the case of 399.2 nm as a function of time. During that 35 minute period the investigated argon ion laser was tuned 3 times to lasing action at 514.53 nm without changing the absorption of the 399.2 nm probing radiation. From the fluctuations of the lock-in signal the error was estimated to ±0.6%.

Similar absorption measurements were also conducted for the ArII transitions 394.43nm, 396.84nm, 426.65 nm, and 442.60 nm. Results

including experimental errors are shown in Figs. 7(b) and 8. Due to the larger absorption of the 426.65 nm and 442.60 nm radiation, fluctuations, and therefore, errors for these lines are somewhat larger. Within the experimental errors we were unable to detect a change in absorption due to lasing action at 514.53 nm in any of the five lines sharing the same upper level 4p $^4D^o_{5/2}$.

While our results clearly do not support the suggestion that self absorption is responsible for the observed quenching effect, a change of Einstein B-coefficients could not be demonstrated either. However, the absorption coefficient κ is connected not only to the lower level population N_l and the Einstein B-coefficient, but also to the upper level population N_u (neglecting statistical weights g_l and g_u) by $\kappa \sim B_{lu} \cdot (N_l - N_u)$.

Therefore, the expected 10% decrease of $B_{399.2\ nm}$ could have been masked by the 20% depopulation of the upper level population n_u.

III. THE EFFECT OF RABI OSCILLATIONS ON THE EMERGENT INTENSITIES

The intense laser field changes the wavefunctions of the involved levels by dressing the states and inducing Rabi oscillations. An interesting suggestion has been made regarding the role of the Rabi oscillations in the experimental observations.[5] Rabi oscillations cause a reduction in intensity of all the spontaneous emission lines from the upper lasing level, however, this reduction is constant for all the lines and cannot, in itself, account for the A-value dependence of the reduction factors. A second effect is that the Rabi oscillations also cause the emission line profile to be split and this, in principle, changes the opacity. Since the 442 nm line is more heavily absorbed in the discharge than the 399 nm line it is suggested that a reduction in opacity could preferentially increase the emergent 442 nm emission compared

to the 399 nm line and account for the observations without the need to postulate quenching of the A-values. The issues here are (i) whether the observed 442 nm/399 nm intensity ratio shows any dependence on opacity, (ii) whether the change in opacity due to the Rabi splitting is large enough to be detected experimentally in the emergent lineshapes, and (iii) whether the expected change in opacity due to the Rabi splitting is quantitively sufficient to account for the quenching As mentioned earlier, experiments were done on three different argon ion discharges of length 1.57, 1.2, and 0.9m, which also differed considerably in 514.53 nm output power (9W, 3.5W, and 2W, respectively). Of course, opacity effects would be expected to play a larger role in the longer discharge but experimentally, all lasers yielded the same apparent depopulation when compared at the same intra-cavity intensity. As detailed above, the change in opacity due to Rabi splitting could not be detected in the transmission of emission from a second argon ion discharge through the first discharge.

A. Line profile measurements

High resolution line shape measurements have been performed by replacing the photomultiplier in Fig. 1(a) by the setup shown in Fig. 1(c). Line radiation of interest was selected by the SPEX monochromator and uniformly expanded by a telescope. A piezo electrically driven plane Fabry-Perot interferometer (Burleigh Model RC-43) was used to scan the line profiles. For 442.6 nm radiation e.g., the free spectral range of the Fabry-Perot was set to 50 GHz and its finesse at 442 nm was measured to be 18 (the finesse was limited to 18 as the dielectric mirrors were not optimized for this wavelength). The measured ArII 442.6 nm line profiles are compared in Fig. 9 for the cases of non-lasing (S_{NL}) and lasing (S_L) of the 514.53 nm laser line. Both profiles agree

in shape within the experimental errors (± 0.5 GHz). In Fig. 10 the integral to peak height ratio and the FWHM of the 442.6 nm emission line is plotted vs. 514.53 nm lasing power. Similar results were found for the 426.65 nm transition. Figures 9 and 10 clearly demonstrate, that any change in the line profiles due to Rabi splitting are negligibly small. Nevertheless, to determine if a small (undetectable) change in the line profile could still play a role in the measurements, modelling of the radiative transfer in the discharge was performed.

B. Modelling of Radiative Transport

The emission lines in the discharge are broadened by a number of factors. For the 442 nm line:

1) Doppler broadening of 4-5 GHz arises from the ion temperature in the discharge of ~3000°K-5000°K.[11]
2) There is an axial magnetic field in the discharge of 0.14 Tesla[12] which causes the line to be Zeeman split into two groups of sub-components separated by 6 GHz.
3) The line is Stark broadened by the plasma electrons by about 1 GHz.[11]
4) The presence of the intra-cavity laser field of ~5 kW cm^{-2} causes a Rabi splitting of 2 GHz.
5) The emergent line profiles are broadened by opacity, particularly the 442 nm line.
6) The experimental line profile in Fig. 9 results from the convolution of all these factors with the Fabry-Perot instrumental function of approximately 2 GHz.

The intra-cavity field will broaden the line profile which will reduce the opacity and, hence, the opacity broadening. Any line broadening mechanism

which distributes the line strength away from the wavelength region of maximum opacity will in principle broaden the emergent line profile and increase the emergent intensity. The model was constructed to estimate the magnitude of this effect. A complete solution of the radiative transfer problem including all the line broadening factors and the radiation field is difficult. There are, however, features of the experimental situation which permit simplification of the general problem. First of all, the narrow diameter and high aspect ratio of the argon ion discharge (length/diameter ~50) means that nearly all of the 442 nm emission escapes radially so that the 442 nm radiation field is decoupled from the populations. The transport of the 442 nm radiation along the discharge can be modelled by simple absorption as the chance of an absorption event leading to re-emission in the direction of observation is negligibly small ($\sim 10^{-4}$). The emergent intensity will be most sensitive to changes in the line profile in the wavelength region where the optical depth is $\tau \sim 1$ (the line core is saturated and the far wings are of low intensity). For a Voight profile this region of the line shape is Lorentzian for the present opacity. Thus, the model treats the case of a Lorentzian profile that is split by the Rabi effect and the effect of opacity is modelled by simple absorption along the discharge.

Let us consider the emission from a small volume element a dx in a cylindrical discharge of cross sectional area, a, and total length, L, located a distance x from one end. The normalized emission line profile is $\emptyset_\nu$ so that the emission dE_ν, from dx at frequency ν is given by:

$$dE_\nu = N_u A \emptyset_\nu a \, dx \, d\vartheta/4\pi. \qquad (1)$$

where N_u is the upper state population, A the radiative transition probability (taken to be constant for the purposes of this model) and $d\vartheta$ is the solid angle

observed. Since the monochromator entrance slit was 1.7 m from the laser, $d\vartheta$ was assumed to be constant over the length of the discharge. The line profile of Lorentzian width Γ, and Rabi splitting Ω, is given by:

$$\emptyset_\nu = \frac{1}{2\pi}\left\{ \frac{\Gamma/2}{(\nu - \nu_0 - \frac{1}{2}\Omega)^2 + (\Gamma/2)^2} + \frac{\Gamma/2}{(\nu - \nu_0 + \frac{1}{2}\Omega)^2 + (\Gamma/2)^2} \right\}. \qquad (2)$$

The intensity from the volume element a.dx emerging from the x=0 end of the discharge is:

$$dS_\nu = dE_\nu \exp(-\kappa_\nu x). \qquad (3)$$

where κ_ν is the absorption coefficient (related to the emission line profile, $\emptyset_\nu$ through detailed balance). Integrating along the length of the discharge we obtain the emergent line profile:

$$\begin{aligned} S_\nu &= \int_0^L dS_\nu \\ &= N_u A \emptyset_\nu a \, (d\vartheta/4\pi) \int_0^L \exp(-\kappa_\nu x)\, dx \\ &= N_u A \emptyset_\nu a \, (d\vartheta/4\pi)\, (1/\kappa_\nu) \{1 - \exp(-\kappa_\nu L)\}. \end{aligned} \qquad (4)$$

A range of parameters were modelled. The most relevant case comprised the comparison of a Lorentzian profile 5 GHz in width (FWHM) with two 5 GHz Lorentzian profiles, separated in frequency by 2 GHz (corresponding to the Rabi splitting). The value of the absorption coefficient κ_ν, was obtained from the experimental absorption data where the 15% transmission of the 442 n.m. line from a second argon ion discharge through the first was measured in the absence of lasing. The second discharge was assumed to have a 5 GHz

Lorentzian emergent line profile, J_ν, and the transmission, integrated over the line profile, obtained from:

$$J^{out} / J^{in} = \int J_\nu^{in} \exp(-\kappa_\nu L)\, d\nu \; / \; \int J_\nu^{in}\, d\nu = 15\%. \qquad (5)$$

The value of the 442 nm line center optical depth obtained in this way was $\kappa_0 L = 10.7$. Figure 11(a) shows the emission line profiles with and without the 2 GHz splitting and the corresponding emergent line profiles. The effect of the 2 GHz splitting is that the width of the emergent line profile increases by 1.4% and the intensity increases by 0.9%. This is a very small effect. Using a 442 nm line center optical depth based on a 10 GHz instead of 5 GHz linewidth for the second discharge resulted in a 0.5% increase. For comparison simply increasing the width of the Lorentzian emission profile from 5 GHz to 7 GHz leads to an 16.5% increase in the emergent line width and 14.7% increase in output intensity. The intensity in the far wings of a Lorentzian profile scales with Γ and, hence the emergent intensity increases with Γ. In contrast a 2 GHz splitting inside a 5 GHz Lorentzian has an effect at line center but the change in the line wings is negligible. Since the line center is saturated anyway there is little effect on the emergent intensity. This is illustrated in Fig. 11 (b) and (c) which shows the ratio of the emission and emergent line profiles with and without the Rabi splitting.

The above model is based on a Lorentzian doublet split by the Rabi frequency [Eq. (2)]. A rigorous theoretical lineshape for the experimental conditions is not available. Alternative expressions for the power broadened lineshape under different conditions may be found in Ref. 9 (eqn. 2.119) and Ref. 13 [Eq. (15)]. In all cases the main effect of power broadening is to change the profile near the line center and not in the far wing. In the experiment

changes in the $\tau \approx 1$ region of the line wing have the strongest influence of the emergent intensity and this is 5-10 GHz from line center (i.e., about 3-5 Ω) for the 442 nm transition so we do not expect more accurate line profiles to change the overall picture.

In conclusion, Rabi splitting of the 442 nm emission line profile will lead to an increase in the emergent line intensity. However, both experiment and modelling show that this effect is much too small to explain the observations. Thus, quenching of the A-coefficients remains the only explanation.

IV. SUMMARY

We have presented further evidence for the change of Einstein's A-coefficients for spontaneous transitions from the upper laser level of an argon ion laser discharge due to the presence of the high-intensity laser flux. Extensive checks were made which ruled out other explanations. Since the emission from the discharge is optically thick, concerns were raised about the role of opacity in the measurements. Absorption measurements using a second argon ion laser showed no change in absorption due to lasing. The 442 nm line profile was measured at high resolution in order to detect any changes in opacity due to Rabi splitting in the intense laser field. Any such changes were below the measurement sensitivity of ±3%. Computer modelling of the effect of Rabi splitting on the emergent line profile confirmed that the effect was negligible. The results of all these measurements clearly exclude a change in self absorption as an explanation for the observed quenching effect.

ACKNOWLEDGMENTS

A large part of this work was made possible by S. Lyon and R. Miles who loaned some of the necessary lasers. We thank them, H. Griem and J. L. Schwob for stimulating discussions. We thank N. Tkach for his able technical assistance.

One of us (F. Aumayr) also gratefully acknowledges financial support by the Austrian Fonds zur Förderung der Wissenschaftlichen Forschung, Project No. J0308P. This work was supported by Advanced Energy Projects, Department of Energy.

(a) Institut für Allgemeine Physik, Technische Universität Wien, A-1040 Wien, Austria.

(b) Also at Princeton Plasma Physics Laboratory, Princeton University, Princeton, NJ 08544 USA.

References

1 Y. Chung, P. Lemaire, and S. Suckewer, Phys. Rev. Lett. **60**, 1122 (1988).

2 Y. Chung, H. Hirose, and S. Suckewer, Phys Rev. A. **40**, 7142 (1989).

3 F. Aumayr, J. Hung, and S. Suckewer, Phys. Rev. Lett. **63**, 1215 (1989).

4 Y. C. Chen and J. L. Lebowitz, Phys.Rev. A **41**, 2127, (1990).

5 H. Griem, submitted to Phys. Rev. Lett.

6 W.L. Wiese, M.W. Smith, and B.M. Miles, *Atomic Transition Probabilities - Na through Ca*, NBS National Standards Reference Data Series- 22 (U.S. GPO, Washington, D. C. 1969) Vol. 2.

7 R.J. Rudko and C.L. Tang, J. Appl. Phys. **38**, 4731 (1967)

8 W.B. Bridges and A.N. Chester, Appl. Opt. **4**, 573 (1965)

9 R. Loudon *The Quantum Theory of Light* (Clarendon, Oxford, 1983), 2nd ed., pp 63 and 307.

10 T.T. Johnston, Appl. Phys. Lett. **17**, 161 (1970)

11 R. C. Sze and W. R. Bennet, Phys. Rev. A **5**, 837, (1972)

12 L. Spinnetti, Coherent Inc., Private communication.

13 H. R. Griem, Phys. Rev. A, **40**, 3706 (1989).

Figure Captions

Fig. 1. Experimental setups used for (a) emission, (b) absorption, and (c) line profile measurements (see text).

Fig. 2. Partial ArII energy level diagram with transition probabilities in units of 10^7 s^{-1}.

Fig. 3. Measured ArII emission spectra in the spectral region 442.0 - 443.2 nm and 398.8 - 399.6 nm, respectively. Full curves have been measured without lasing, broken curves with 9 W lasing at 514.53 nm. Only the 399.205 nm and the 442.601 nm emission line show a measurable decrease in intensity with lasing.

Fig. 4. Ratio of measured spontaneous emission intensities at full (approx. 5 kW/cm^2 at 514.53 nm) intra-cavity power density S(P=Pmax) to emission intensities at zero intra-cavity power density S(P=0) as a function of Einstein A-Coefficient A_{ij} of respective transitions from the common ArII 4p $^4D^\circ_{5/2}$ upper level.

Fig. 5. Ratio of the spontaneous emission intensities of the 399.2 nm to the 442.6 nm transition as a function of intra-cavity (514.53 nm) laser power density P. (The signal ratio has been normalized to 1 at P=0).

Fig. 6. Lasing (L) to non-lasing (NL) ratio of measured spontaneous emission intensities (=apparent depopulation) for polarization components parallel and perpendicular to the laser polarization direction, respectively. Measurements were performed by inserting a rotatable Glan-Taylor prism polarizer into the beam path. Results for different polarizer orientations are identical within the experimental errors.

Fig. 7. a) Transmitted fraction of the 399.2 nm probing radiation as a function of time. No change in signal is notable when the argon ion laser is tuned to lasing action at 514.53 nm. The two straight lines correspond

to a ±1% region around the average value.

b) Transmitted fraction of the 442.6 nm probing radiation as a function of time. No change in signal is notable when the argon ion laser is tuned to lasing action at 514.53 nm.

Fig. 8. Measured change in transmission through the absorbing argon plasma for the five probing lines from the common ArII 4p $^4D^\circ_{5/2}$ upper level. The results indicate no change within the experimental errors.

Fig. 9 Comparison of ArII 442.6 nm line profiles as measured with the Fabry-Perot interferometer for the cases of non-lasing (o) and full power lasing (●) of the 514.53 nm laser line. Both profiles agree in shape but, of course, differ in absolute scale.

Fig. 10 Integral to peak height ratio (●) and full width at half maximum (o) of the 442.6 nm emission line vs. 514.53 nm lasing power.

Fig. 11 Results of the modelling calculations: (a) 5 GHz Lorentzian emission line profiles with (●), and without (o) the 2 GHz splitting and the corresponding emergent line profiles with (×), and without (+) the 2 GHz splitting; (b) ratio of the emission line profiles with and without the 2 GHz splitting; and (c) ratio of the emergent line profiles with and without the 2 GHz splitting.

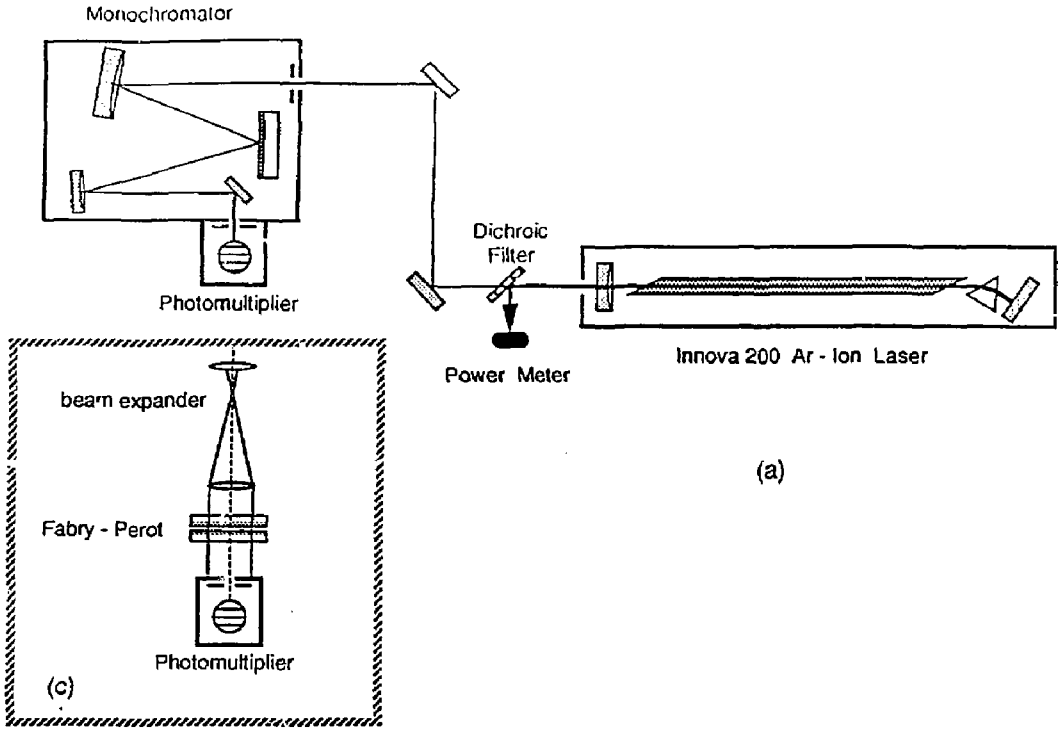
Monochromator
Photomultiplier
Dichroic
Filter
Power Meter
Innova 200 Ar - Ion Laser
(a)
beam expander
Fabry - Perot
Photomultiplier
(c)

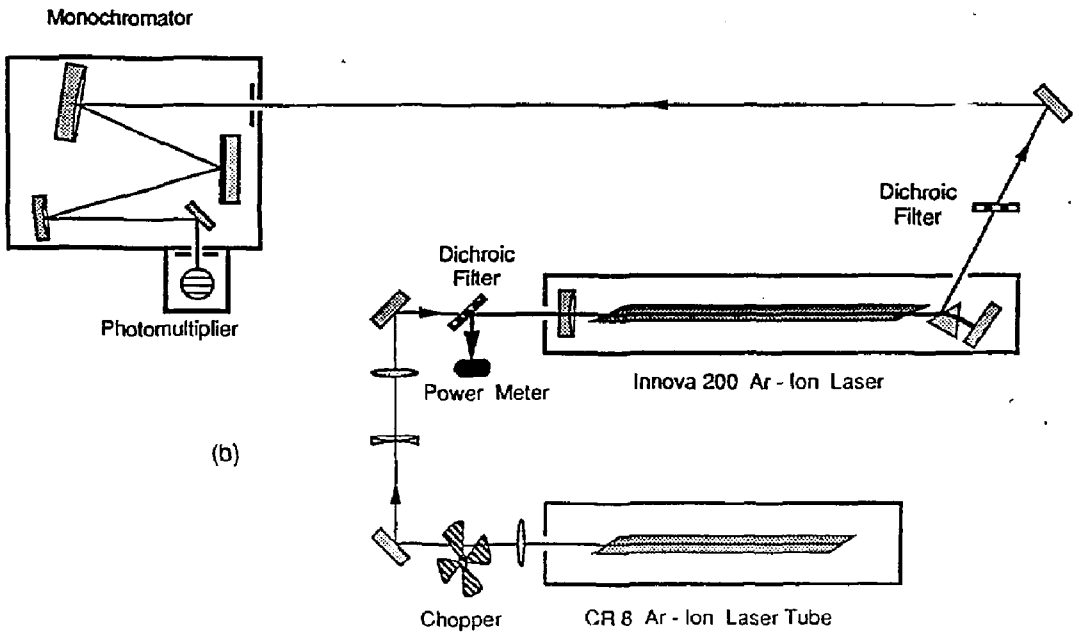
Monochromator
Photomultiplier
Dichroic
Filter
Dichroic
Filter
Power Meter
Innova 200 Ar - Ion Laser
(b)
Chopper
CR 8 Ar - Ion Laser Tube

Fig. 1

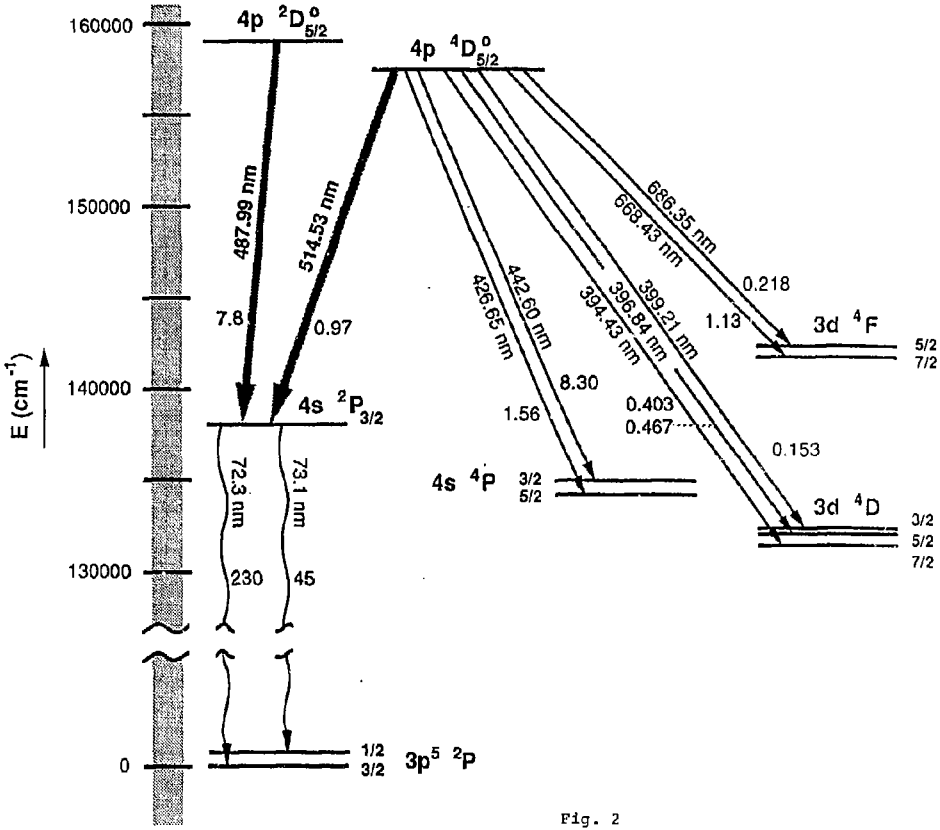
160000
150000
140000
130000
0
E (cm^{-1})
4p $^2D^o_{5/2}$
4p $^4D^o_{5/2}$
487.99 nm
514.53 nm
7.8
0.97
4s $^2P_{3/2}$
72.3 nm
73.1 nm
230
45
1/2
3/2
3p^5 ^2P
426.65 nm
442.60 nm
8.30
1.56
4s ^4P 3/2
5/2
686.35 nm
668.43 nm
399.21 nm
396.84 nm
394.43 nm
0.218
1.13
0.403
0.467
0.153
3d ^4F 5/2
7/2
3d ^4D 3/2
5/2
7/2

Fig. 2

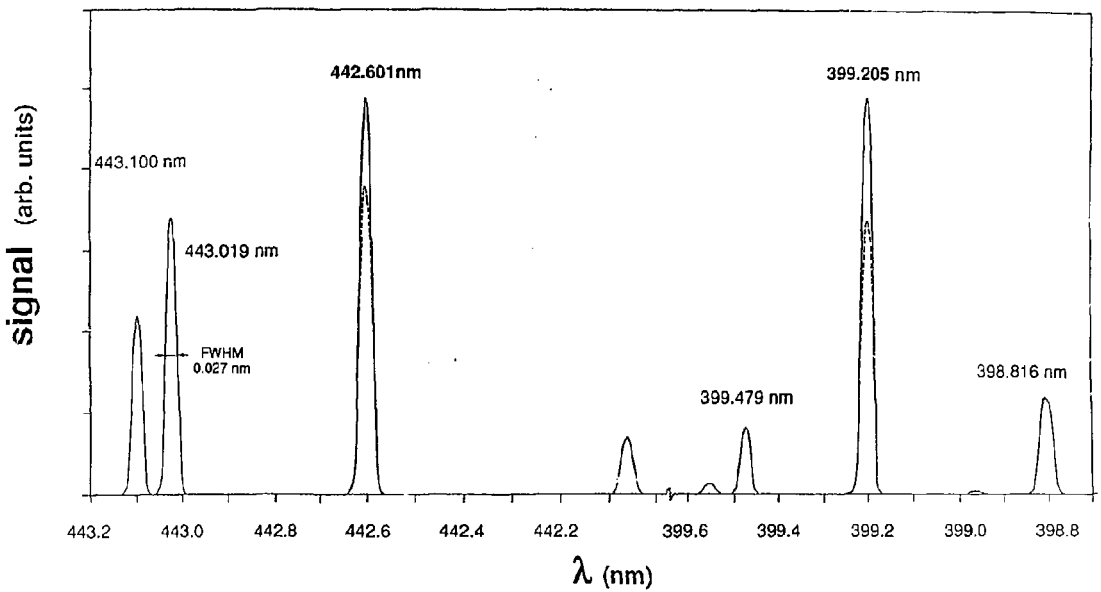
signal (arb. units)
442.601nm
399.205 nm
443.100 nm
443.019 nm
FWHM
0.027 nm
399.479 nm
398.816 nm
443.2
443.0
442.8
442.6
442.4
442.2
399.6
399.4
399.2
399.0
398.8
λ (nm)

Fig. 3

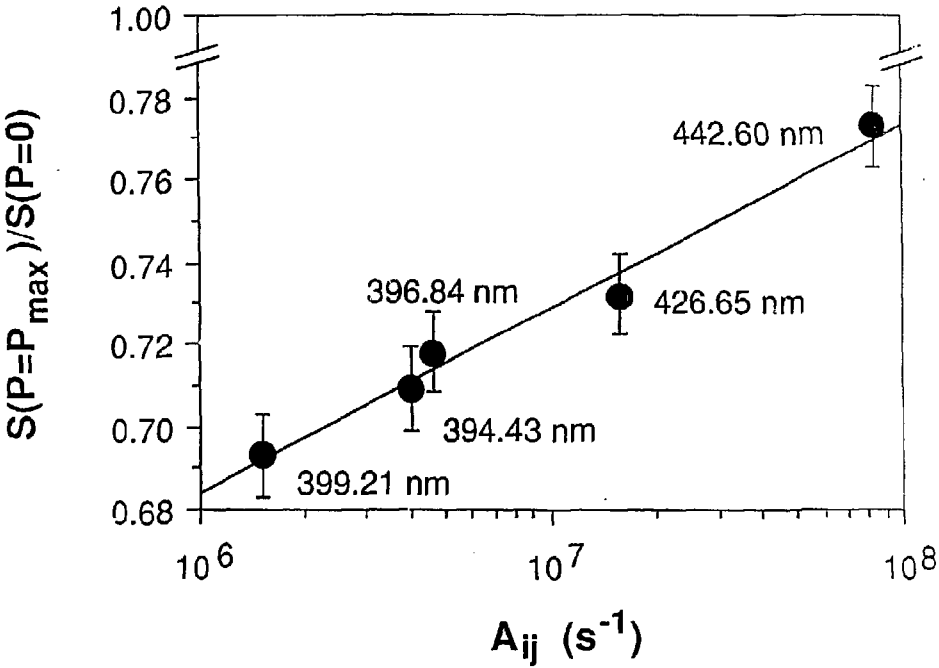
1.00
0.78
0.76
0.74
0.72
0.70
0.68
S(P=P max)/S(P=0)
442.60 nm
396.84 nm
426.65 nm
394.43 nm
399.21 nm
10 6
10 7
10 8
A ij (s -1)

Fig. 4

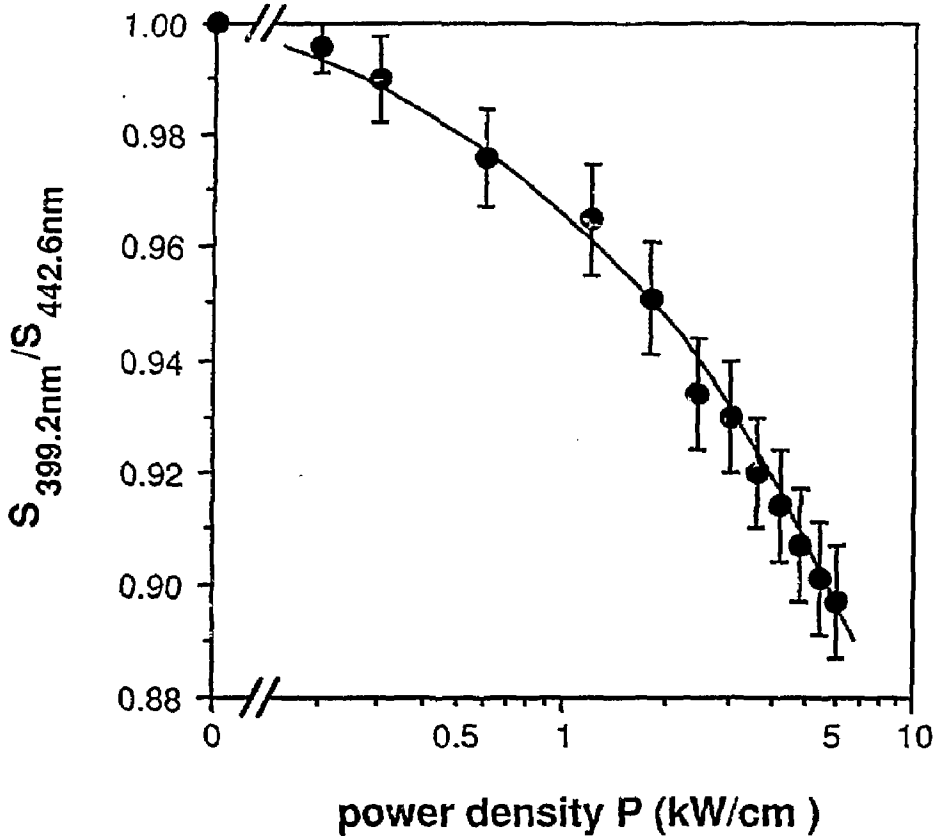
1.00
0.98
0.96
0.94
0.92
0.90
0.88
0
0.5
1
5
10
$S_{399.2nm}/S_{442.6nm}$
power density P (kW/cm)

Fig. 5

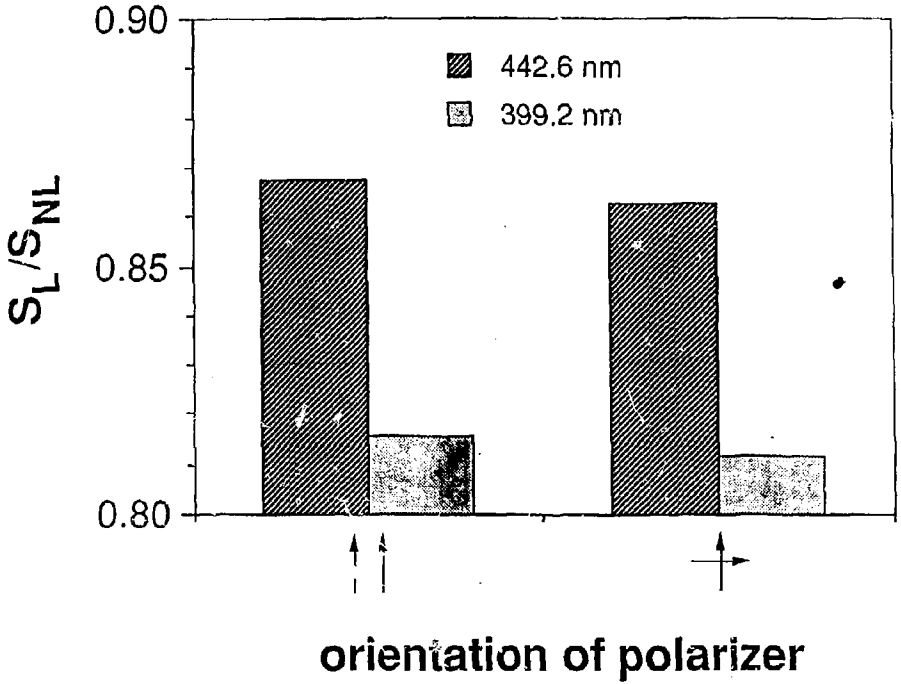

Fig. 6

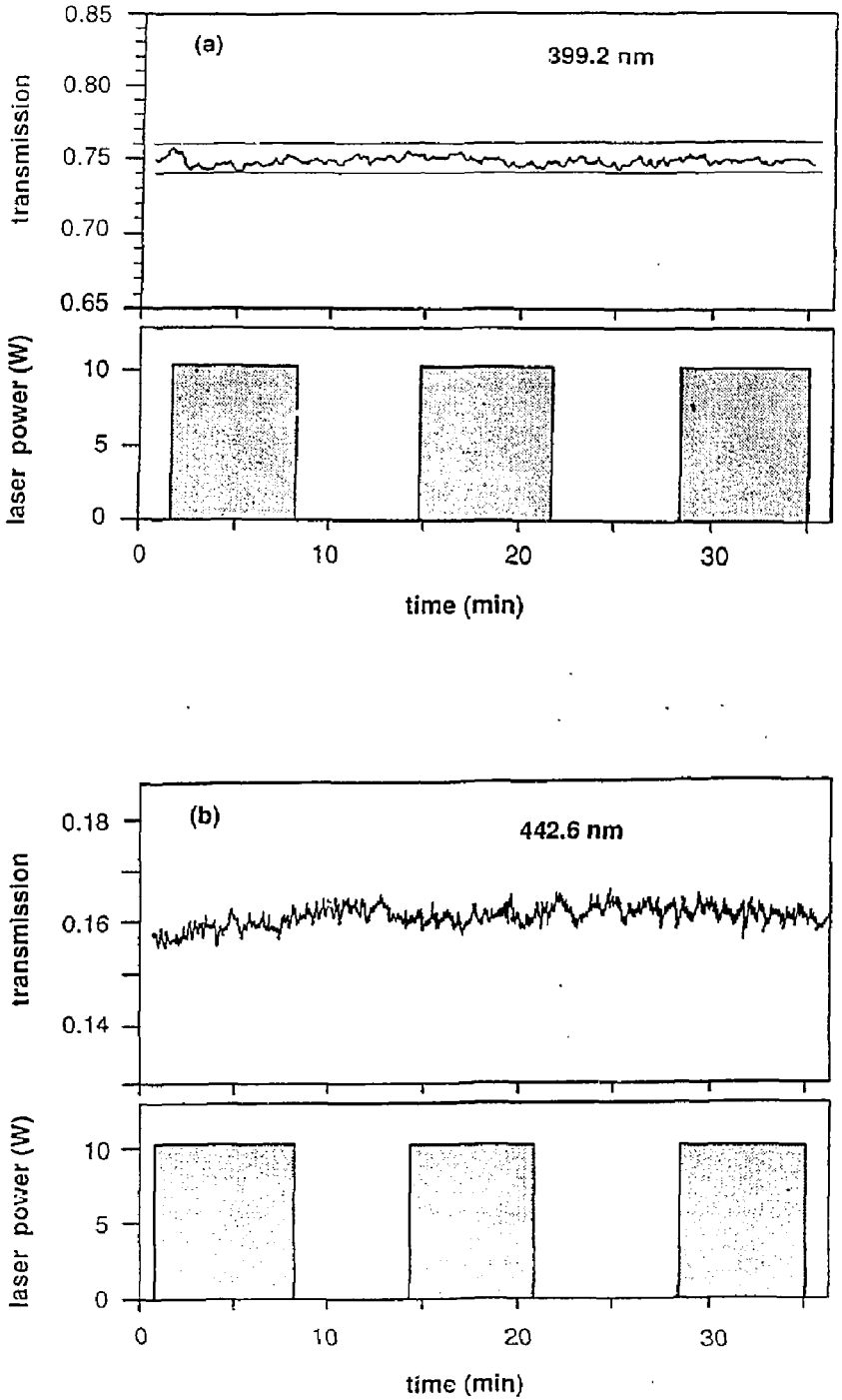
(a)
399.2 nm
transmission
0.85
0.80
0.75
0.70
0.65
laser power (W)
10
5
0
0
10
20
30
time (min)
(b)
442.6 nm
transmission
0.18
0.16
0.14
laser power (W)
10
5
0
0
10
20
30
time (min)

Fig. 7

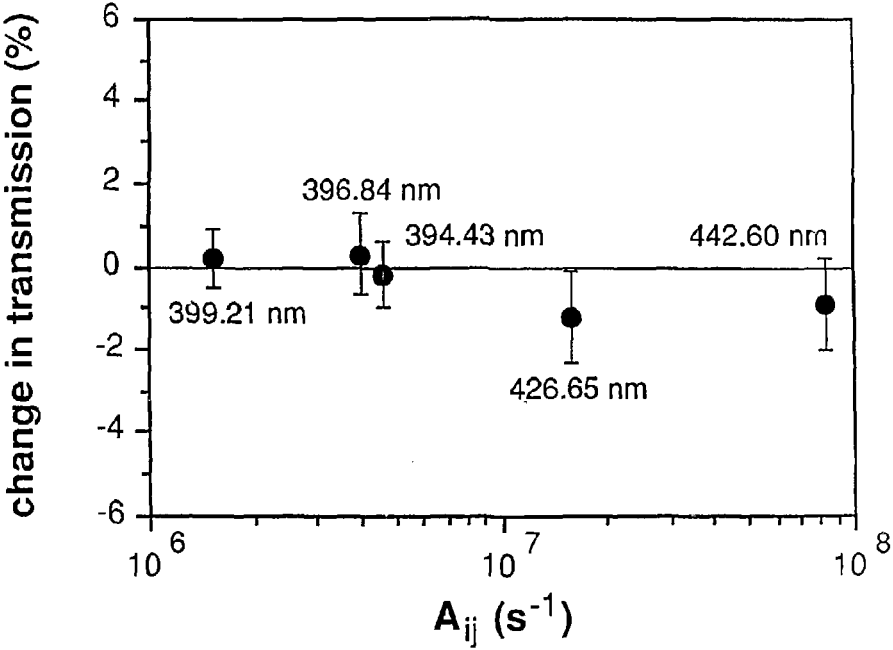
change in transmission (%)
6
4
2
0
-2
-4
-6
396.84 nm
394.43 nm
442.60 nm
399.21 nm
426.65 nm
10 6
10 7
10 8
A ij (s -1)

Fig. 8

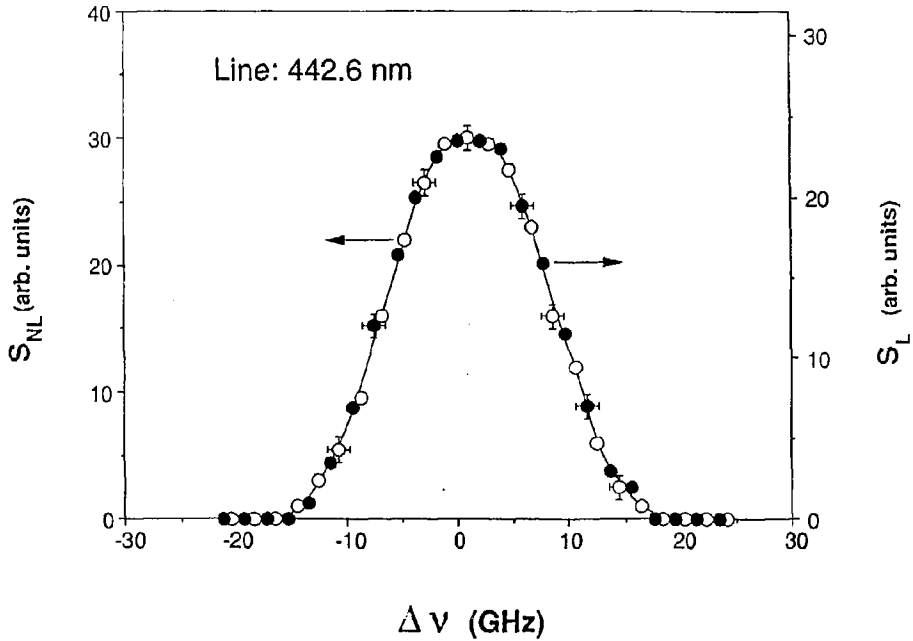
Line: 442.6 nm
S_{NL} (arb. units)
S_L (arb. units)
$\Delta\nu$ (GHz)
40
30
20
10
0
-30
-20
-10
0
10
20
30

Fig. 9

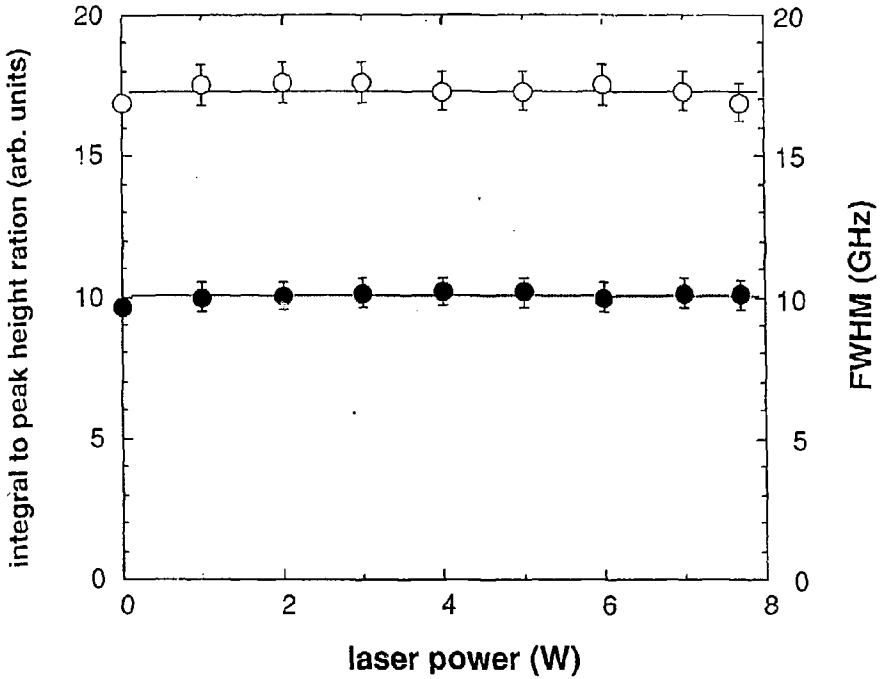
integral to peak height ration (arb. units)
FWHM (GHz)
laser power (W)
0
5
10
15
20
0
2
4
6
8

Fig. 10

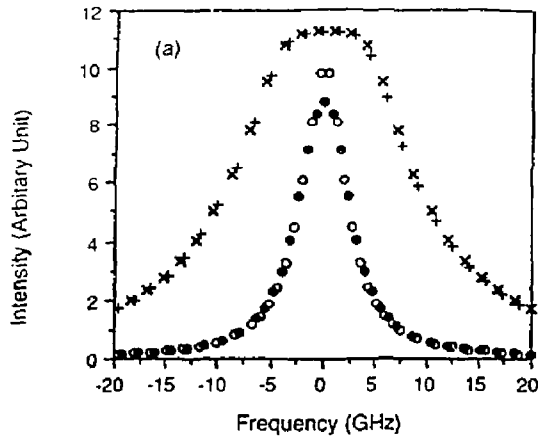
(a)
Intensity (Arbitary Unit)
Frequency (GHz)

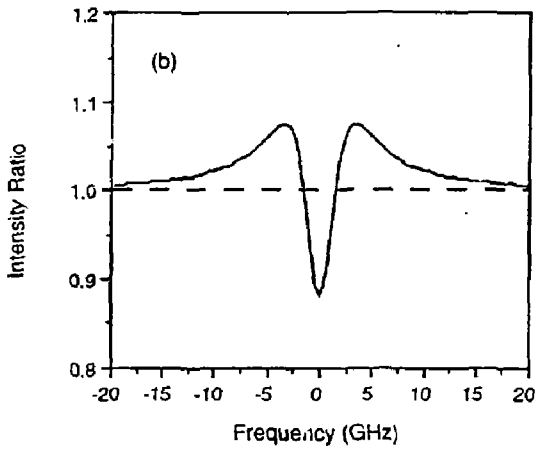
(b)
Intensity Ratio
Frequency (GHz)

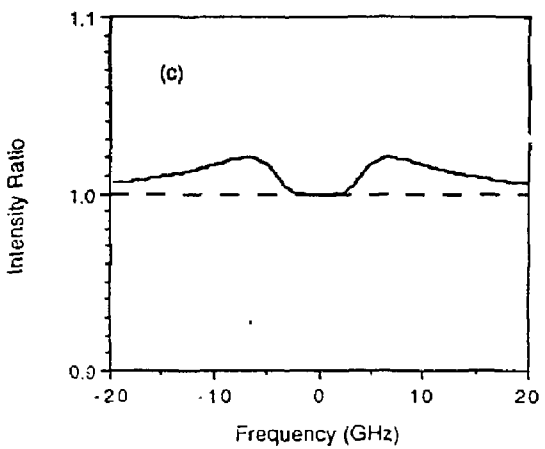
(c)
Intensity Ratio
Frequency (GHz)

Fig. 11